



HAL
open science

Human performance in the Traveling Salesman Problem is influenced by spatial scale

C. Doussot, S. Muflih, J. Mailly, M.M. Müller, N. Boeddeker, Mathieu Lihoreau

► **To cite this version:**

C. Doussot, S. Muflih, J. Mailly, M.M. Müller, N. Boeddeker, et al.. Human performance in the Traveling Salesman Problem is influenced by spatial scale. 2025. <hal-05376892>

HAL Id: hal-05376892

<https://hal.science/hal-05376892v1>

Preprint submitted on 21 Nov 2025

HAL is a multi-disciplinary open access archive for the deposit and dissemination of scientific research documents, whether they are published or not. The documents may come from teaching and research institutions in France or abroad, or from public or private research centers.

L'archive ouverte pluridisciplinaire **HAL**, est destinée au dépôt et à la diffusion de documents scientifiques de niveau recherche, publiés ou non, émanant des établissements d'enseignement et de recherche français ou étrangers, des laboratoires publics ou privés.



HAL Authorization

1 **Human performance in the Traveling Salesman Problem**
2 **is influenced by spatial scale**

3 C. Doussot^{1,*}, S. Muflih², J. Mailly¹, M.M. Müller², N. Boeddeker², M. Lihoreau^{1,*}

4 ¹ Univ. Toulouse, CNRS, Research Center on Animal Cognition (CRCA-CBI),
5 Toulouse, France

6 ² Bielefeld University, Department for Neurobiology, Germany

7 *Corresponding authors: cha.doussot@gmail.com, mathieu.lihoreau@utoulouse.fr

8

9 Abstract

10 Like many other animals, we humans frequently face complex route optimization
11 problems when planning journeys between multiple locations. Several strategies can
12 be employed to approach such Traveling Salesman Problems. However, these may
13 be strongly constrained by spatial scales, for instance if the goal is to navigate in a
14 supermarket, in a city, or across a continent. Here, we monitored the route
15 optimization performances of human subjects collecting objects in a video game
16 simulating 3D environments at various spatial scales. Unexpectedly, route
17 optimization performances peaked at intermediate spatial scales, where participants
18 could use global optimization strategies. At very large and very small spatial scales,
19 however, participants predominantly employed less efficient local optimization
20 strategies. At the very large scale, the considerable distances between objects
21 prevented them from being seen all at once, making global planning difficult. At the
22 very small scale, participants reported having chosen the shortest path, although they
23 did not. This mismatch between perceived and actual performances suggests
24 suboptimal alternatives were sufficiently short to be considered equivalent to the
25 optimal route. Spatial scale thus strongly influences route planning in human
26 navigators and may determine the spatial behaviors of a wide range of animals facing
27 similar routing problems in their everyday lives.

28 Keywords: navigation, multi-destination routes, route optimization, Traveling
29 Salesperson Problem, virtual reality.

30

31 Introduction

32 Animals exploiting patchily distributed resources commonly need to revisit key
33 locations in their environments while minimizing travel costs. Finding the shortest
34 route passing through multiple places is analogous to a formal computational
35 challenge known as the Traveling Salesman Problem (TSP), a NP-hard problem that
36 rapidly becomes intractable(1) as the number of locations increases(1), but for which
37 heuristic algorithms can approach solutions at low computational costs(2).

38 Humans and many other animals have been described to apply some of these
39 heuristics when asked to solve TSPs by drawing a single stroke linking all dots
40 arranged on a 2D representation (figural TSP)(3–5) or visiting locations across an
41 experimental environment (navigational TSP)(6–8). Local strategies determine the
42 route to follow during only a few steps ahead, like moving to a nearest neighbor
43 target (NN strategy(9)) or grouping visits to nearby targets (Cluster strategy(10, 11)).
44 By contrast, global strategies consider the overall layout and planning of the full route
45 to be used, which generally improves the optimization performance. For example,
46 humans tend to use a convex hull (CH) strategy when presented with figural TSPs(3,
47 12–14). They first draw a mental border connecting the outermost targets and
48 gradually pull it inward to include the dots within the polygon shape. This behavior
49 was also observed in monkeys(15), rats(16) and bees(17) in navigational TSPs.
50 However, navigators often appear to combine local and global strategies(5, 18–20)
51 by which first, a coarse approximation of the route is established globally and then
52 refined locally, potentially reducing the cognitive load for the animal(11, 21).

53 Since TSPs can occur at any spatial scale, distance perception by animals may
54 have a strong impact on the strategies employed and the resulting optimization
55 performances(22, 23). In large-scale environments where target locations are far
56 from each other and potentially hidden by clutter, individuals may rely more on local
57 strategies(7, 24). By contrast, in small-scale environments, where all target locations
58 are visible at once, individuals may use global planning. While the comparison of
59 human performances in a figural TSP (on a piece of paper) and a navigational TSP
60 (in a room-sized environment) suggests individuals use similar heuristics across
61 spatial scales (24), the two tasks involve very different behaviors. They may thus rely
62 on different cognitive mechanisms, including complex visual and attentional
63 processes, as well as spatial memory(22).

64 Here, we tested the effect of spatial scale on navigational TSP by monitoring
65 the route optimization performances of human subjects collecting 10 objects (chests)
66 in a 3D virtual environment (a Viking village) (25, 26). The participants were asked to
67 repeat the task in the same array of objects but at different spatial scales, so that the
68 distances between the collectibles either decreased or increased while keeping the
69 rest of the visual setting stable. In these conditions, we expected better optimization
70 performances in small environments that allowed global planning, compared to larger
71 environments where local strategies were more practical. Contrary to our

72 expectations, we found that the optimization performance peaked at intermediate
73 spatial scales.

74 Results

75 Variation in route preferences at three different scales

76 In a first experiment (Exp1), we asked the participants to collect 10 chests and return
77 to the start location, while taking the fewest steps as possible (**Fig. 1A**). Each
78 participant repeated the task in four arrays of chests: a circular arrangement (one
79 side-bias control), and three experimental configurations (Exp1-C1, C2, C3), at three
80 spatial scales each (S: small (1:2), M: medium, L: large (3:2)) (**Fig. 1D**). In these
81 environments, we measured the utilization of local versus global route optimization
82 strategies by analyzing the first direction (left-right) chosen by the subjects upon
83 leaving the start location N1 (**Table 1**). As expected, we found no side preference by
84 the participants in the control array (Binomial test: corrected p values >0.05 for scale
85 S, M, and L; statistics = 0.60, 0.54, 0.63). However, this was not the case in the three
86 experimental configurations.

87 In the first configuration (Exp1-C1), participants tended to move first to their right
88 (toward chest N10) and collect the cluster of 5 chests (N6-10) rather than moving to
89 the nearest neighbor chest (N2). This preference was the most frequent at the small
90 spatial scale (S) and decreased with increasing scale sizes (**Table 1**). In this
91 configuration, several possible routes (sequences of chest collection) were close to
92 optimal (of less than 1% length difference with the shortest possible route).
93 Participants used a range of these near-optimal routes (R1, R2, and R3). Their
94 frequency of usage varied with spatial scale, suggesting different strategies were
95 used to collect the chests within the cluster (**Fig. 1B**).

96 In the second configuration (Exp1-C2), participants showed no clear preference
97 between moving left toward the nearest neighbor chest (N2) or right toward a more
98 distant chest (N10; **Table 1**). The optimal route (R1) was preferentially used at all
99 spatial scales (**Fig. 1B**).

100 In the third configuration (Exp1-C3), participants showed no clear preference
101 between moving left toward the nearest neighbor chest (N2) or right toward two more
102 distant chests (N10 and N9; **Table 1**). This configuration required participants to
103 decide when to integrate the internal chest N4 into their routes. The optimal route
104 (R1) was preferentially use at all spatial scales, and especially at the medium spatial
105 scale (M), where it was observed in 77% of the trials (**Fig. 1B**).

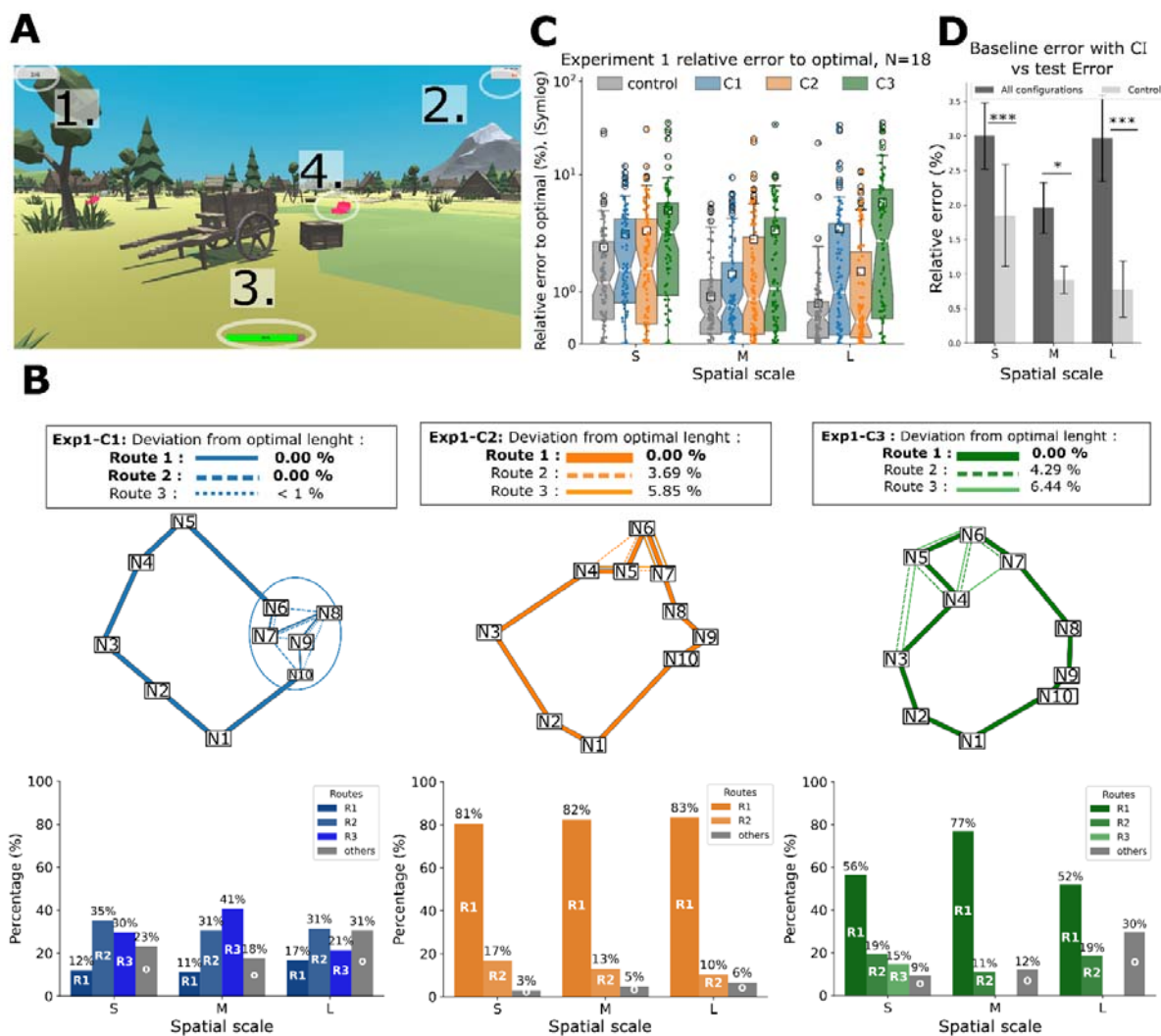
106 The overall performance of participants, computed from the deviation of their
107 walking trajectories from the shortest possible path (i.e., the relative error) (**Fig. 1D**),
108 shows a complex relationship with spatial scale. Contrary to our expectations, there
109 was no systematic decline in optimization performance with increasing spatial scale.
110 In fact, the opposite was observed in the Control condition as well as in Exp1-C2,
111 where the relative error decreased with increasing spatial scale (GLMM with M scale

112 as reference; $\beta=-0.474$, $SE=-0.11$, $t=-4.286$, $p < 0.001$). Responses to spatial scale in
 113 Exp1-C1 and Exp1-C3 differed. In Exp1-C1 the relative error shows a quadratic
 114 relationship with spatial scale (quadratic component; $\beta=0.486$, $SE=0.27$, $t=1.792$, $p <$
 115 0.1), indicating that participants deviated less from the optimal path length at the
 116 medium spatial scale. Relative errors in simpler configurations that could be solved
 117 by moving in a circle (Control and Exp1-C2), may indicate a baseline level of error
 118 attributable to motor imprecision within the video game or an incautious player
 119 behavior at a smaller scale. This effect was further magnified because of the
 120 normalization process to percentages that we applied. For each spatial scale, the
 121 relative error was different from the error-baseline defined by the Control (Mann–
 122 Whitney U test; S and L: $p < 0.001$, M : $p < 0.05$, and differences in GLMM model
 123 estimates see **Table S1**), suggesting that motor imprecision of the participants alone
 124 cannot account for the elevated relative error observed, particularly at the smallest
 125 and largest spatial scales S and L (**Fig. 1C**). Relative errors also decreased over time
 126 as participants gained experience with the game. Across session order, the model
 127 revealed a significant reduction in relative error ($\beta = -0.036$, $SE = 0.013$, $t = -2.68$, p
 128 < 0.01) and a significant decrease across trial numbers ($\beta = -0.11$, $SE = 0.026$, $t = -$
 129 4.13 , $p < 0.001$).

130 The fact that human subjects performed better at the medium spatial scale by
 131 employing more often the optimal route, suggests they changed strategies across
 132 scales. However, the three configurations used in our game did not enable us to
 133 precisely characterize this change.

134 **Table 1:** Left - Right preferences across environments and spatial scales. For all conditions, chest N2
 135 is the nearest neighbor from the start location N1. The last column presents Chi-test results assessing
 136 side-bias across environments and spatial scales. Significant differences from the binomial test testing
 137 for a side preference for each scale are represented in bold. We used 0.05 as the level of significance
 138 after Holm-Bonferroni correction at the configuration level. Levels of significance are *** <0.001 , ** <0.1 ,
 139 * <0.5 , . <0.1 .

Config.	Left start (N2)	Right start (other)	Stats	Overall Preferred side
Exp1-C1	S: 37.0%* , M: 42.6%, L: 46.3%	S: 63.0%* , M: 57.4%, L: 53.7%	$X^2 = 3.9$, df = 2, p >0.5	Right side: Binom. test: s =0.58, p < 0.01
Exp1-C2	S: 58.3%, M: 57.4%, L: 54.6%	S: 41.7%, M: 42.6%, L: 45.4%	$X^2 = 0.32$, df = 2, p > 0.5	Left side: Binom. test: s =0.56, p < 0.01
Exp1-C3	S: 50.0%, M: 51.9%, L: 57.4%	S: 50.0%, M: 48.1%, L: 42.6%	$X^2 = 1.28$, df = 2, p > 0.5	No preference Binom. test: s =0.53, p > 0.05
Exp2-C1	XS: 37.0% , S: 40.0%, M: 43.0%, L: 51.0%, XL : 43.0%	XS: 63.0% , S: 60.0%, M : 57.0%, L: 49.0%, XL : 57.0%	$X^2 = 3.59$, df = 4, p > 0.5	Right side: Binom. test: s =0.57, p < 0.001
Exp2-C2	XS: 48.0%, S: 38.0%, M : 47.0%, L: 48.0%, XL : 36.0%*	XS: 51.0%, S: 62.0%, M: 52.0%, L: 51.0%, XL : 64.0%*	$X^2 = 6.27$, df = 4, p > 0.5	Right side: Binom. test: s =0.55, p < 0.01



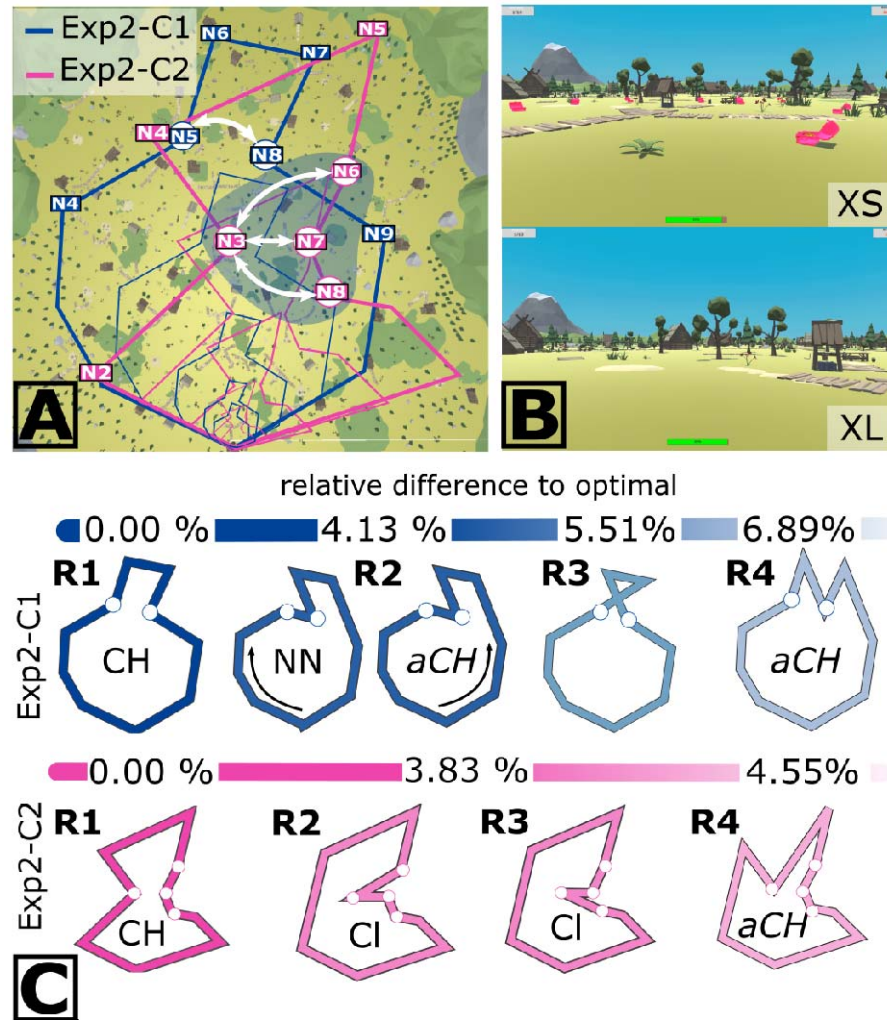
141

142 **Figure 1: Experiment 1 (N = 18).** **A) In-game view.** 1. The inventory indicates the number of chests collected. 2.
 143 The number of steps executed from the start. 3. The stamina bar, which decreases as the number of steps
 144 increases. 4. Item to collect with a glowing pink texture, indicating it has not been visited yet. **B) Relative error to
 145 the optimal trajectory at different spatial scales.** Boxplots of the relative error scaled in symmetric Log due to
 146 highly skewed data towards zero. A color represents one configuration (see legend caption). The white squares
 147 are the means. **C) Boxplot of Baseline-error distribution (derived from control) versus test-error (C1, C2,
 148 and C3) at different spatial scales.** Error bars indicate the Confidence interval (95%). Level of significance
 149 between error distributions is indicated with * <0.05, ** <0.01, *** < 0.001. **D) Schematic representation of
 150 Configurations 1, 2, and 3** (in blue, orange, and green, respectively): N1-N10 are nodes representing chests.
 151 The optimal (R1) and suboptimal topological routes are represented with their associated relative error to optimal
 152 %. The color gradient indicates the relative error to optimal, except for Exp1-C1, where all routes are below <1%.
 153 Optimal route R1 is the thick solid line, the second-best route the dashed line (R2), and finally the third route
 154 the thin line (R3). If more than 4 nodes are close to each other, we regroup them within a circle (cluster). **D) Route
 155 choices made by participants in experiment 1.** Proportions of the different routes (sequences of chest
 156 collection) observed at the different spatial scales (S, M, L) for the three configurations Exp1-C1, Exp1-C2, and
 157 Exp1-C3 from left to right. The colors refer to the routes as defined in the upper graph. Routes performed less
 158 than 10% of the time are grouped under the Light Grey bar (and referred to as others).

159

160 **Conflict between global and local heuristics at five different scales**

161 To further explore how human navigators may change optimization strategies across
 162 spatial scales, we conducted a second experiment (Exp2) using two new
 163 configurations (C1 and C2), in which a direct conflict arose between a global strategy
 164 (the convex hull strategy, CH) and one of two local strategies (cluster or nearest
 165 neighbor, NN). We enhanced the assessment of performance variation across spatial
 166 scales by adding two more scales using the previous M scale as a benchmark (XS,
 167 S, M, L, and XL, **Fig. 2A & B**). Moreover, the possible routes inside each
 168 configuration were more different from the optimal route than in Experiment 1 (**Fig.**
 169 **2C**).



170

171 **Figure 2: Design of Experiment 2. A) Game map with all optimal routes** for the two configurations of nodes
 172 (chests) at five spatial scales. Broader lines indicate the XL scale. White arrows indicate heuristic conflict
 173 locations. For configuration 1 (blue line), there is a possibility for an NN transition between N5 and N8. For
 174 configuration 2 (pink line), there is a possibility for a cluster strategy between N3 and any of N6, N7, or N8 (cluster
 175 in shaded area). **B) In-game views at the two extreme spatial scales:** Top, smaller scale (XS); bottom, larger
 176 scale (XL). **C) Four best routes** for Exp2-C1 and Exp2-C2 and associated optimization strategy. A color gradient
 177 shows the percentage difference from the optimal route (R1). Dark blue (optimal) to light blue (non-optimal) for
 178 C1, and Pink to light pink for C2. CH stands for convex hull strategy, "aCH" for alternative CH, NN for nearest
 179 neighbor strategy, and finally Cl for Cluster strategy.

180 We designed Exp2-C1 to test the conflict between the usage of an NN and a
181 CH strategy. Participants used the NN transitions between N5–N8 (b) and N7–N9 (e)
182 differently depending on spatial scale. At the small spatial scale S, transitions (b) and
183 (e) were less often used than at the other four spatial scales (N5-N8: $X^2 = 5.83$, $df =$
184 1 , $p < 0.05$; N7-N9: $X^2 = 8.53$, $df = 1$, $p < 0.003$) (**Fig. 3A**). Corroboratively, the CH
185 transitions showed the opposite trend (N7-N8: $X^2 = 3.32$, $df = 1$, $p < 0.1$; N8-N9: $X^2 =$
186 2.19 , $df = 1$, $p > 0.05$). To further clarify the strategies employed during transition (b),
187 we differentiated between the two directions: movement from N5 to N8 and from N8
188 to N5, as the latter does not necessarily reflect an NN strategy but results from
189 initially choosing the most distant chest (N7). Movements from N5 to N8 (i.e., NN
190 strategy) were less frequently observed at medium spatial scales (frequencies: XS:
191 22.22%, S: 5.75%, M: 8.06%, L: 17.24%, XL: 12.12%), whereas movements from N8
192 to N5 (i.e. start with most distant chest) were less frequent at small spatial scales
193 (XS: 6.06%; S: 8.05%; M: 16.13%; L: 16.09%; XL: 14.14%). At spatial scale S, the
194 optimal route (CH strategy) was used most frequently, in 74.4% of the trials (**Fig. 3A**),
195 with R2 as the second most used route (**Fig. 2C**). At the largest spatial scales (L and
196 XL), participants used a more diverse set of routes, with 41–46% of trials involving
197 sub-optimal routes.

198 In Exp2 - C2, the transition frequencies that varied the most between spatial
199 scales were those created to impose conflict between the CH strategy (R1) and the
200 Cluster strategy (**Fig. 3B**). The transition N2-N4 (c), associated with a misuse of the
201 CH strategy and resulting in clustering the chest N3 with the N6 to N8 chests, was
202 more often used at the two extreme spatial scales ($X^2 = 12.86$, $df = 1$, $p < 0.001$).
203 Occurrence of transitions (b) and (d) varied in consequence of transitions (c). The
204 use of N1-N10 (a), N4-N5 (f), N3-N6 (e) decreased with increasing spatial scale. The
205 optimal route was the most frequently used at medium spatial scales S (54.0% of
206 trials) and M (45.7% of trials) (**Fig. 3B**). Participants used a broader range of routes
207 at large spatial scales: 70% of them were not from the three best ones at the XL
208 spatial scale (**Fig. 3B**).

209 Across both environments, participants showed a bias to start routes by
210 turning right. In Exp2-C1, this meant they did not preferentially begin by collecting the
211 nearest chest to the start location (N2), while in Exp2-C2, they typically started with
212 the chest that led to the cluster (**Table 2**), which is consistent with the patterns
213 observed in Experiment 1.

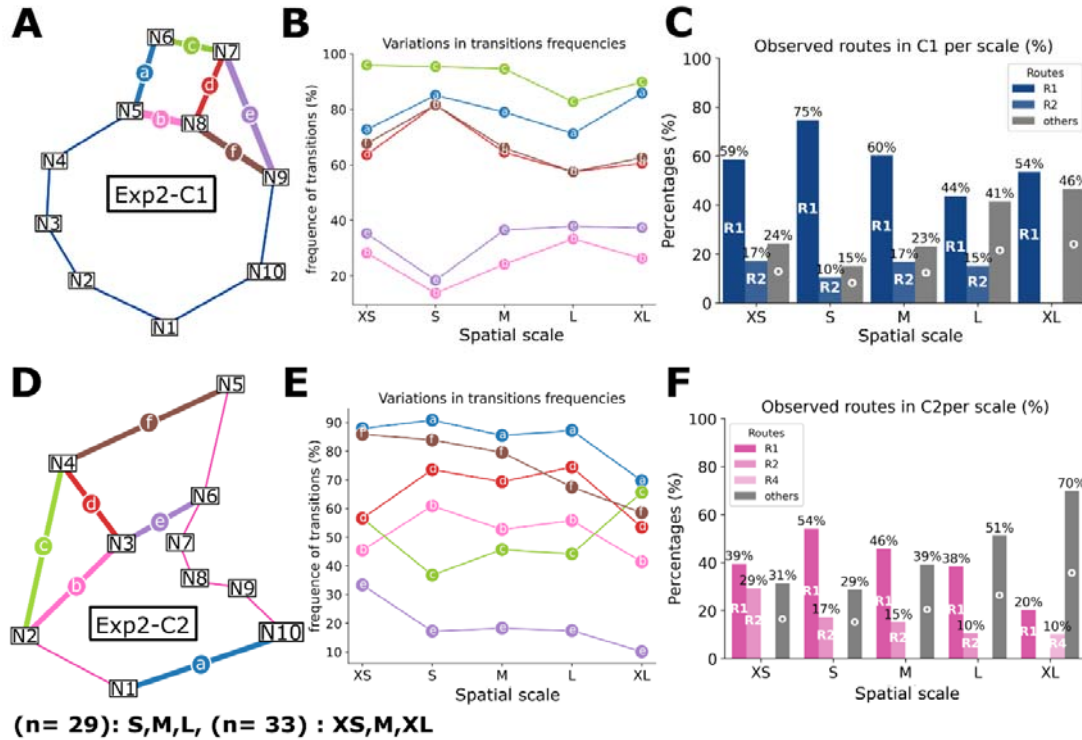


Figure 3: Route choices in Experiment 2 A) route choice in Exp2-C1. A is a schematic of the transitions with the highest variability across spatial scales. B) Occurrence of transitions at each spatial scale. Letters and associated colors refer to the color scheme in A. C is a bar chart of the different routes observed at different spatial scales. Route nomenclature fits the one in Figure 1, and the color scheme the relative error to optimal (from darker optimal to lighter less optimal). D) route choice in Exp2-C2. All the subplots E and F follow the same characteristics of the first row.

214

215 We then examined whether the scale-dependent pattern observed in the
 216 relative error of experiment 1 (Fig. 1B) extends to the more extreme spatial scales in
 217 experiment 2. The change in spatial scale showed significant predictive power of the
 218 error relative to optimal, following a linear component and a quadratic component
 219 (Table 2). Like in experiment 1, errors peaked at the extreme scales, indicating a
 220 quadratic relationship. There was no significant effect of the spatial configuration (C1
 221 and C2). In addition, including inter-individual differences and reducing the number of
 222 predictors to gaming habits and trial number in the model increased the marginal R^2
 223 (see Table S2 for tested models). Finally, increasing trial numbers and gaming habits
 224 significantly reduced the deviation of participants from optimal (Table 2; $p < 0.001$).
 225 Our selected model (Table 2) was then validated against other models that showed
 226 no significance through Likelihood ratio tests and AIC (AIC = 7587.6, $X^2 = 3.7684$, df
 227 = 3, $p = 0.29$). Our results and a simplified version of the fitted model are given in
 228 Fig. 4B.

229 **Table 2: Model predicting the relationship between the relative error from optimal and spatial**
230 **scale.** Model : AIC = 7587.6, BIC = 7622.4. The model follows a quadratic curve, with its linear term
231 representing the scale and the quadratic term being $I(\text{Scale}^2)$, where participants' IDs serve as a
232 random effect. All predictors are reported in the Variables column. β : estimate, SE: standard error, t:
233 the t-value, and p: p-value.

Model: Relative error ~ Scale + $I(\text{Scale}^2)$ + Trial number + Gaming habits + (1 ID), family = Gamma (link function = log)				
Variables	β	SE	t	p
(Intercept)	4.27418	0.21109	20.249	< 0.001
Scale (linear term)	-0.72802	0.11150	-6.529	< 0.001
$I(\text{Scale}^2)$ (quadratic term)	0.13812	0.01838	7.514	< 0.001
Trial number	-0.18699	0.03340	-5.599	< 0.001
Gaming habits	-0.22826	0.04086	-5.587	< 0.001

234

235 Because Experiment 2 offered clear optimal routes distinct from suboptimal ones,
236 we examined the frequency of optimal route usage by the participants using a
237 GLMM. After the exclusion of unnecessary predicting variables (see **Table S3**), the
238 two chest configurations gave different responses. We compared two models; one in
239 which the relation between the response rate and the spatial scale differed across
240 configurations (with configurations as interaction effect: AIC = 1399.6, BIC 1444.5, df
241 = 9, $R^2 = 18.6\%$) and one where the performance was lower for Exp2-C2, but the
242 effect of scale remained consistent across configurations (AIC = 1401.3, BIC
243 =1436.2, df = 7, $R^2 = 17.5\%$). We chose the earlier model because it had fewer
244 degrees of freedom, and the Likelihood-ratio test only suggested a marginal
245 improvement from using the complex model's prediction ($X^2 = 5.6436$, df = 2, p <
246 0.1).

247 Spatial scale significantly predicted optimal route usage with a linear (p < 0.1)
248 and a quadratic component (p < 0.01) (**Table 3**). Gaming habits and trial numbers
249 increased the observation of optimal route usage. Participants had significantly
250 higher optimization performance in the first configuration (Exp2 – C1) than in the
251 second one (Exp2 – C2) (p < 0.001, **Table 3**). When accounting for these differences,
252 it increased the conditional R^2 by 7.7% (Marginal $R^2 = 9.8\%$, Conditional $R^2 = 17.5\%$).
253 The distribution of optimal route usage and a simplified version of the fitted model are
254 represented in **Fig. 4B**.

255 The results of Experiment 2 thus overall confirmed that the relative error and the
256 optimal route usage follow the same non-linear pattern indicated by Experiment 1 at
257 the extreme spatial scale.

258 **Table 3:** Model predicting the relation between optimal route usage and the spatial scale. Model: AIC = 1401.3, BIC = 1436.2. The model follows a quadratic curve with its linear term being the scale and the quadratic term being $I(\text{Scale}^2)$ with participants' ID as a random effect. All predictors are reported in the Variables column. This table reports β : estimate, SE: standard error, t: the t-value and p: p-value

Model: Optimal route observation ~ Scale + I(Scale ²) + Configuration + gaming habits + trial nb. + (1 ID), family = Binomial (logit)				
Variable	β	SE	z	p
(Intercept)	-0.65607	0.43506	-1.508	0.132
Scale (linear term)	0.43770	0.25566	1.712	0.087
I(Scale ²) (quadratic term)	-0.11085	0.04203	-2.638	0.008
Conf. C2	-0.81363	0.13225	-6.152	< 0.001
Gaming habits	0.17984	0.06332	2.840	0.005
Trial Number	0.19449	0.08043	2.418	0.016

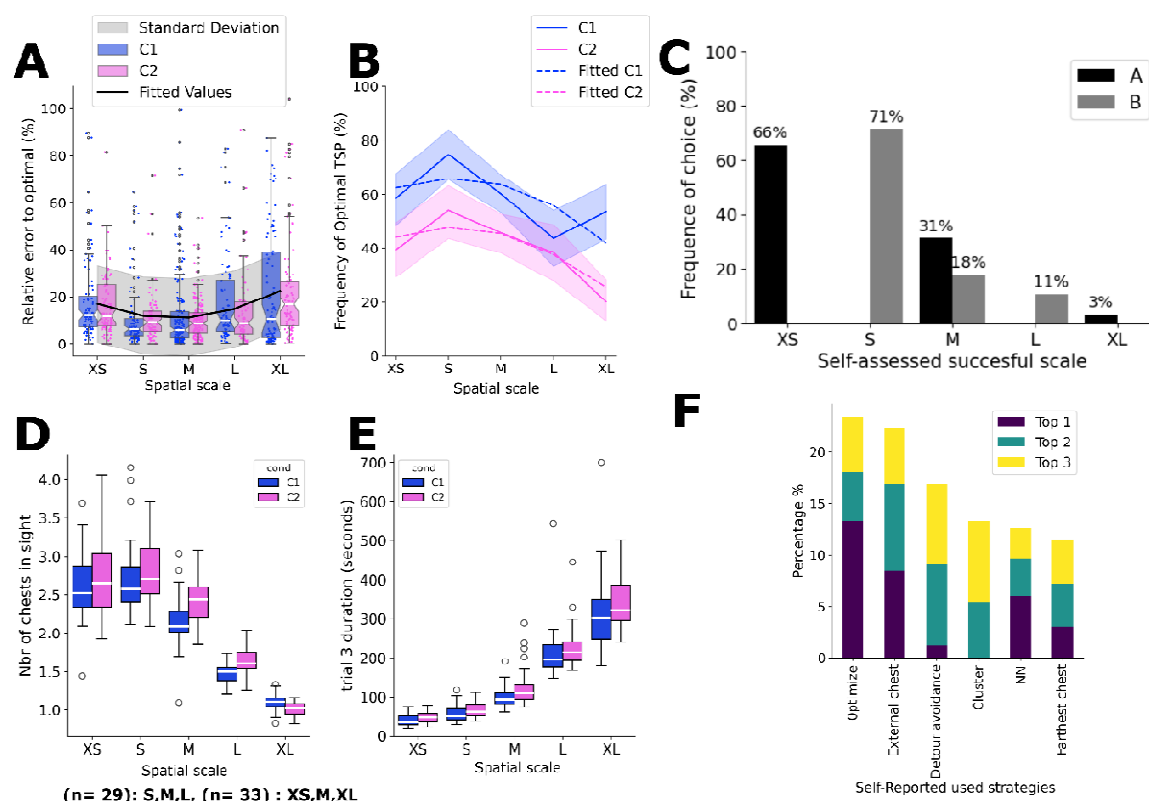


Figure 4: Route optimization performance in Experiment 2. A) Relative error to the optimal path at different spatial scales. Colors of boxplots indicate the configurations C1 and C2 (see legend). The median is in white. Dots are individual data. The black line represents a simplified version of the selected GLMM model (formula = error ~ scale + I(scale²)) and the grey shading represents residual deviation. **B) Frequency of optimal route usage** for each configuration with its corresponding standard deviation. The dashed lines represent the fitted values for the simplified version of the selected GLMM (formula = TSP correct ~ scale + I(scale²) + configuration). **C) Proportions of self-assessed use of the optimal route.** **D) Average estimated number of chests in sight** during the last trial at any scale and configuration. The number of chests in sight was computed based on the participant's orientation and position in their last trial (trial number 3). **E) Average duration of a game session** in seconds for the different configurations and at each scale at trial number 3. **F) Proportions of self-assessed used strategies.** See in S3 for the detailed formulation of the different criteria present in the feedback survey.

262 Discussion

263 Using a video game, we demonstrated that humans solving a navigational TSP
264 performed better at intermediate spatial scales compared to very small or large ones.
265 This contradicts our initial assumption that global route optimization strategies,
266 associated with higher performances, are primarily used in small-scale environments
267 where all the target locations are visible at once. Instead, we found a complex, scale-
268 dependent relationship between optimization strategies and task performance.

269 As initially expected, in the video game chest visibility decreased at larger scales
270 (Text S5, LM: $\beta=-0.45$, SE = 0.007, $t =-61.803$, $p < 0.001$). This hindered global
271 planning and led participants to make incremental decisions based on local
272 considerations, often resulting in longer routes than the optimal one at large spatial
273 scales (**Fig. 4B**). Our result is consistent with the idea that humans are unlikely to
274 represent a sizeable environment within a unique allocentric reference frame(27) and
275 rather use a dynamic representation where remote places are updated intermittently,
276 and nearby ones are continuously maintained(28). Our observations are also in line
277 with reports that the human sense of direction worsens when planning across several
278 regions of interest versus within a single region(29).

279 However, in contrast to our expectations and despite the good chest visibility,
280 participants also performed poorly on the smallest spatial scales. In these conditions,
281 most participants relied on local strategies, such as favoring the collection of chests
282 placed inside a cluster (Exp2-C2) or moving between nearest-neighbor chests (Exp2-
283 C1). To our knowledge, no study has reported larger errors in distance discrimination
284 and in path integration at a small scale compared to larger ones(30–32), thus calling
285 for alternative explanations. We suggest that at the smallest spatial scales tested in
286 the second experiment, the perception of optimality by the participants becomes
287 ambiguous. In that regard, the surveys filled by the subjects just after being tested
288 are insightful. Variation in perception of optimality can be understood, for instance, in
289 a shopping context when customers do not exclusively reduce their traveled distance
290 but seek to minimize their time carrying heavy weight(33). Similarly, an individual may
291 choose the fastest route over the shortest one: just as a car driver might prefer a
292 slightly longer road with no traffic light to a shorter route with many. In our surveys,
293 participants overestimated their performance for small scales and underestimated it
294 at medium scales (**Fig. 4E**). At the smallest spatial scale (XS), most participants
295 collected chests in a suboptimal sequence and thus exceeded the optimal travel
296 distance. This suggests they did not deliberately settle for “satisficing” (i.e., good
297 enough) solutions(14, 34) or used quicker and less cognitively demanding
298 optimization strategies (i.e., local strategies). Instead, they may have perceived their
299 route as optimal because the task felt quick and feasible, as all chests were visible
300 and routes were overall short. Performance peaked at intermediate spatial scales,
301 reflecting a trade-off: as scale increased, feasibility decreased while the benefit for
302 precise judgment of the optimal route (e.g., saving time) increased. This non-linear
303 pattern mirrors the predictions of resource-rational analysis (35), according to which

304 humans allocate cognitive effort in proportion to the expected gains of optimization
305 (expected utility(36)), leading to maximal performances when cognitive costs and
306 task benefits are balanced. Finally, at the smallest spatial scale, object proximity may
307 have initiated a “crowding-effect”: all items were visible but categorized as equally
308 beneficial(37, 38). Because all distances were short, participants may have
309 considered various routes equally satisfying, despite their actual differences, leading
310 to a choice overload and suboptimal solutions (39). This also raises the question of
311 the extent to which relative distance can be perceived on a smaller scale, a problem
312 that should be specifically addressed in future studies.

313 Strategy reporting in the surveys further revealed a mismatch between self-
314 perception and actual routing behavior (**Fig. 4F**). If using the optimal route was
315 described as the main strategy by most participants, many reported that they
316 attempted to “*take the external chests to then go to the ones inside*” and “*avoid*
317 *turns,*”; two behaviors related with the CH strategy(40). Although the NN strategy
318 enabling individuals to follow the optimal path for many transitions, “*going to the*
319 *closest chest*” was represented in the top three in less than 15% of the surveys. The
320 behavior “*collect chests that appear grouped together*”, akin to the cluster strategy,
321 was also underrepresented, given that our results highlight a preference towards
322 node clusters. It is possible that some participants anticipated local strategies to be
323 inherently less efficient for solving TSPs and chose not to report it. This gap between
324 perception and behavior was also noted in an earlier study through analyses of the
325 verbalizations of human subjects tasked to solve the TSP(41). This mismatch could
326 reflect that these strategies may not be “competing” but rather complementary.

327 Since the discovery of place cells in the rodent brain(42), investigation of
328 navigation’s neural basis often takes place in room-sized environments, where the
329 idea of a perfect mental map(43) can easily be supported. (44–46). Yet, our findings
330 demonstrate that the spatial scale of such tasks is an important factor to consider, as
331 certain scales could be more sensitive to detecting navigation impairments than
332 others. Overall, our data illustrate the importance of accounting for spatial scales
333 when studying spatial cognition. Researchers are now investigating how the
334 neurological components facilitating a cognitive map can be used for larger-scale
335 planning (43). For example, a study suggests a gradual shift from concrete to
336 abstract processing as reflected in brain activity(47), where environments grow
337 beyond the sensory horizon. We argue that navigational TSP is well-suited for
338 studying how neural processes may be at play at different spatial scales during path
339 planning and spatial learning, even outside the human scope(27), like in rodents,
340 birds, and insects. Bees, for instance, are known to optimize their foraging paths
341 when exploiting flower meadows at larger spatial scales than in smaller environments
342 (48, 49). Ultimately such fundamental advances could lead to new applications in the
343 societal domain. For instance, navigation assays based on navigational TSP and
344 fluctuation in spatial scales could help enhance the early detection of

345 neurodegenerative diseases, such as Alzheimer's disease, where deficits in spatial
346 navigation are among the first cognitive symptoms (44–46).

347

348 Material and methods

349 Participants

350 We ran two experiments with voluntary subjects (see details in **Table 4**). In
351 Experiment 1, we tested 18 healthy participants aged between 19 and 40 years
352 (mean = 29.27 years, SD = 6.17) in 2023. Participants were recruited from the local
353 community through word-of-mouth and acquaintances from Germany and Jordan. In
354 Experiment 2, we tested 62 healthy adults from France, Germany, the UK, and the
355 USA, aged between 18 and 55 years old (mean = 30.27 years, SD = 7.36) in 2024.
356 The participants were selected through word of mouth. We also advertised the
357 project on the university campuses of Toulouse (France) and Bielefeld (Germany).
358 The screening included participants' demographics: age and self-reported gender
359 identity. Participants were not involved in the study if they reported any untreated
360 mental or visual disorders. All subjects provided informed consent to participate in the
361 game and complete the final survey. They were informed about the nature of the
362 study, the potential risks and benefits, and their right to withdraw from the study at
363 any time. The data collected in the study were anonymized and stored securely. One
364 participant reported that they could not finish the game due to motion sickness; 6
365 others did not complete the task or made it in several days and were removed to
366 avoid learning biases. The final dataset contained 62 participants. All the participants
367 filled in a survey about personal habits that could influence their performance,
368 including GPS usage, planning practice and video gaming experience(50)

369 Game design

370 For both experiments, we used the same video game created in Unity2021 (Unity
371 Technologies; game available in https://github.com/dousscha/TSP_data_2025). The
372 game interface used to collect the data and create the surveys was made using the
373 Unity Experiment framework toolbox(51), and the game logic was made using the
374 Virtual Navigation Toolbox(52). We used a desktop display similar to previous studies
375 on human navigation(53–56).

376 The game is in 3D and from a first-person perspective. It requires the use of a
377 mouse and keyboard to control the player's movements and views. Using a mouse
378 was strongly encouraged; however, two participants used their touchpad in
379 Experiment 2. The game was designed to simulate a navigation task in a village
380 environment (a free Viking village set from the Unity store) that is considered
381 comparable to a "real-world" scenario, in the sense that it offers realistic visual clutter
382 and landmarks (**Fig. 1A**). The main instruction given to players was to collect the
383 treasure chests optimally in the environment while keeping track of the number of
384 steps taken, and to return to the starting location. There were 10 glowing pink chests

385 scattered throughout the environment, but one was positioned directly at the start
386 location. To assess their own performance, the participants were informed that they
387 could check their step count on the top right of the screen, as displayed in **Fig. 1A**.
388 Furthermore, the game interface displayed a stamina bar that ran low with the
389 number of steps taken. In Experiment 2, the virtual stamina decreased at the same
390 rate for all scales to realistically implement the notion of travel cost. When stamina
391 was below 10%, the bar turned red, and a heavy breathing sound was played. This
392 feature was not implemented in the earlier experiment (Experiment 1), where stamina
393 was normalized to the spatial scale investigated (**Table 4**).

394 We kept the gameplay simple and accessible to a broad audience. The player
395 had to move through the environment with the only constraint that large objects, like
396 houses, could not be crossed. To collect a chest, the player needed to move into its
397 close surroundings (approximately 1 step from its center). The spatial configurations
398 of chests were designed using the center of each chest to compute the optimal route;
399 hence, the circular collection zone around a chest could not be too large, as it would
400 change what route is considered as the TSP solution. When a chest was collected, a
401 sound was displayed, a message appeared on the screen, and the number of chests
402 collected was updated in the left-hand corner of the screen. Furthermore, the color of
403 the chest turned black, but the chest was not removed from the map, so participants
404 would not return to an already visited location. When all the chests were collected,
405 the player was asked through a screen message to return to the start location in
406 order to end the trial. Importantly, the completion of the task was independent of the
407 state of the stamina bar that could be emptied before the player returned to the
408 starting point. During the game, the player's trajectory, chest collection order, and
409 time to complete the task were saved.

410 **Table 4:** Methodological details of the two experiments

	Experiment 1 (2023)	Experiment 2 (2024)
Number of participants	18	62
Duration	$\cong 3\text{h}$	47min11s (SD $\cong 11\text{min}$)
Instructions	Oral, given by the experimenter	Written on the main menu
stamina bar	Correlated with scale	Finite: uncorrelated with scale
Number of configurations	1 control and 3 tests	2 tests
Number of spatial scales	3	5 tested, but only 3 played per participant (game A or B)
Interaction with participants	Participants were asked to speak out their thoughts while navigating.	No interaction with the experimenter. From home.

411

412 Study design

413 Experiment 1

414 We used one control condition (10 chests arranged in a circle) and three spatial
415 configurations (Exp1 C-1, Exp1 C-2, Exp1 C-3) inspired by Blaser and
416 Ginchansky(57) (**Fig. AC**) to test for preferences in optimization strategies at three

417 spatial scales (S, M, and L). The first configuration (Exp1-C1) provided several
418 suboptimal routes whose lengths were close to that of the optimal route (< 1%
419 difference) (**Fig. 1B**). The first and second configurations (Exp1-C1 and -C2) offered
420 a choice between the nearest object (N2) or a cluster of objects (N10) further away
421 from the departure point (N1). In the third configuration (Exp1-C3), participants had to
422 decide when to incorporate the internal node (N4) on their way, following a CH
423 strategy.

424 These tests were conducted in the presence of an experimenter (see details
425 about instructions in Text S1). Before the test, participants received a brief training
426 session to familiarize themselves with the video game and the TSP navigation task
427 (i.e., a demo session where they had to collect six chests arranged in a circle). The
428 experimenter asked the participant to navigate through the village and collect the
429 objects using the shortest route, using as few steps as possible. Participants were
430 instructed to speak out their thoughts while navigating, to describe the strategies they
431 thought they applied to find the shortest route. The experimenter provided guidance if
432 needed during the experiment. After the demo, participants were randomly assigned
433 a configuration and completed it at all three spatial scales in random order before
434 moving on to the next configuration. They were asked to respond to questions in
435 between each TSP exercise, and another series at the end of the experiment (see
436 questionnaire in Text S2).

437 **Experiment 2**

438 Experiment 1 revealed an unexpected quadratic spatial scale effect on the global
439 performance of participants and affected their route choices (**Fig. 1**). We therefore
440 performed a complementary Experiment 2 with two new configurations (Exp2-C1,
441 Exp2-C2), conflicting global and local strategies, and at more spatial scales (XS, S,
442 M, L, XL) to include extremely small and large ones (**Fig. 2A**).

443 Exp2-C1 was used to test the CH and NN strategy. In this configuration most
444 transitions composing the optimal route followed NN transitions, except the transition
445 between N5 and N8, which belonged to the CH route (**Fig. 2A**). At this location, using
446 the shortest transition led to a suboptimal solution of the TSP (R2) (**Fig. 2C**). Yet in
447 R2, moving from N8 to N5 might not be a NN transition if it results from moving to N7
448 from N9 first; in this case the participant may decide to collect first the farthest node
449 or attempt a CH strategy, referred as an alternative CH (aCH) (**Fig. 2C**). The best
450 suboptimal route (R2) was 4.13% longer than the optimal.

451 Exp2-C2 had a cluster of 5 chests positioned on the right of the departure
452 location (**Fig. 2A**). According to previously mentioned strategies, the player could
453 either collect all the chests together using the cluster strategy (R2 and R3) or include
454 the outermost chest of the cluster (N3) while forming the left border of the convex
455 shape (CH strategy) (**Fig. 2A**). Performing the latter would lead to the optimal route
456 (R1). The best suboptimal route among all possibilities following the cluster strategy
457 would lead to a 3.83% deviation from the optimal (R2).

458 Based on the results of experiment 1, where optimal routes were most observed
459 at a medium spatial scale, we tested participants on five spatial scales (326 steps in
460 length). The medium spatial scale was 363 steps long for Exp2-C1 and 418 for Exp2-
461 C2, and the four other spatial scales were two to three times smaller or longer,
462 ranging from XS to XL (**Fig. 2A&B**). To reduce experimental time and the risks that
463 participants abandon the task, they were divided into two groups, each tested on
464 three of the five spatial scales rather than all five. One group of participants was
465 tested at spatial scales XS, M and XL (N = 33) and was asked to download the game
466 A, and the other group played at scales S, M and L (N= 29) in game B. To control for
467 potential learning effects on the TSP performances, the order in which the
468 participants performed the scale was pseudo-randomized. The participants
469 systematically started with Exp2-C1 followed by Exp2-C2 at the same spatial scale.
470 They all had three trials per session (configuration and scale). In total, each of them
471 did 6 sessions, taking on average a total of 47 minutes and 11 seconds (SD \cong 12
472 minutes).

473 Experiment 2 was performed without the supervision of an experimenter. The
474 participants received an email with a link to download a game, A or B, depending on
475 the group they were assigned. The invitation included all the necessary details to run
476 the game: the ID used for later anonymization, the order in which to play the mini
477 games (i.e., a specific combination of configuration and spatial scale, unknown to the
478 player), and a notice to send their data back. The email informed the participants of
479 approximate duration of the experiment (between 50 and 65 minutes) so that they
480 could plan their time accordingly. Upon launching the game, the menu screen
481 indicated the aim of the game, the consent form, and some of the pre-experiment
482 survey questions (see questionnaire in **Text S3**). These questions were asked
483 beforehand to avoid biasing the results due to the experience of playing the game
484 (see full menu screen text in **Text S4**). The players run the demo first, to familiarize
485 themselves with the setup. After, participants played each mini game in the order they
486 were given . At the end, the participants filled out a final survey about their
487 optimization routine and performance assessment (see questions in S3). The
488 questions followed either a Likert-based or a semantic differential-based scoring
489 system(58). The game was available in French and English.

490 Data analysis

491 The raw data are available in https://github.com/dousscha/TSP_data_2025.

492 We studied left-right biases in the routes of participants to explore strategy
493 preferences in Experiment 1 and side preference in Experiment 2. We used an exact
494 binomial-test to test for preferences and a chi-squared test to identify changes in
495 proportions of strategy/side usage due to spatial scale. We further characterized the
496 routes taken by participants across scales in both experiments, focusing on the
497 transitions between chests. To assess variation in frequencies of transition between
498 two chests, we applied chi-squared tests.

499 We then looked at various metrics to describe the participants' performance.
500 Firstly, for both experiments, we measured the relative length deviation between each
501 participant's trajectory and the optimal path (i.e. relative error, F1).

$$502 \quad \mathbf{F1} \text{ Percentage error (\%)} = \frac{(\text{distance travelled} - \text{optimal length})}{\text{optimal length}} \times 100$$

503

504 The optimal route, i.e., the shortest possible route to collect the 10 chests, was
505 first computed based on the route passing through each chest center (i.e., theoretical
506 optimal). However, due to the virtual catchment zone around each chest allowing
507 their virtual collection, the actual optimal path length might be slightly shorter than the
508 computed one. Consequently, the optimal was recomputed from the minimum of all
509 candidates if this one happened to be below our theoretical optimal.

510 Secondly, and only for Experiment 2, because it offered an optimal route that was
511 clearly different from the suboptimal ones (3.83% difference minimum, **Fig. 2**), we
512 reported success in optimally solving the TSP for each trial, i.e., collecting the chest
513 in the optimal order independently of the walked trajectory. Contrary to the error, this
514 metric does not account for any zigzagging movements that could be due to poor
515 gaming habits.

516 We analyzed the data using Python and R. For the performance metrics (relative
517 error and optimal TSP frequency), we fitted GLMMs in R. Initial models included
518 effects of trial number, session order, age, gender, gaming habits, GPS usage,
519 navigation assessment, and optimization practice. Non-predicting variables were
520 removed during model selection. Player ID was also included as a categorical
521 random effect to examine for inter-individual differences. We always tested for the
522 interaction effect of the configurations and the significant predictive variable. Models
523 were selected based on the Akaike Information Criterion (AIC), Likelihood ratios test,
524 and their simplicity (i.e., low degree of freedom). Hence, interactions were removed
525 since they were shown not to be significant and worsen the model simplicity. When
526 necessary, due to the non-linearity of the variables' responses (relative error and
527 optimal TSP solving frequency), we used the spatial scale as a numeric predictor
528 during model fitting, even though we did not assume equidistance in the response
529 relative to increasing scale. We used a gamma distribution with a Log link function for
530 the relative error. While the success of optimal TSP in a trial was either 0 (no optimal
531 TSP) or 1 (optimal solving), we used a binomial distribution for model fitting. To allow
532 for proper model fitting and analysis, outliers were removed using the z-score metric;
533 any results with a z-score above three were removed.

534 **Ethics statement**

535 All experiments were conducted in accordance with the guidelines of the Deutsche
536 Gesellschaft für Psychologie e.V. (DGPs) and approved by the Bielefeld University
537 Ethics Committee. The studies were conducted in accordance with the local

538 legislation and institutional requirements. The participants provided their written
539 informed consent to participate in this study.

540 **Author contributions**

541 CD: Conceptualization, Data curation, Formal analysis, Methodology, Software,
542 Visualization, Writing—original draft, Writing—review & editing. SM:
543 Conceptualization, Methodology, Data curation, Writing—review & editing, JM:
544 Methodology, Writing—review & editing. MM: Software, Writing—review & editing.
545 NB: Project administration, Supervision, Writing—review & editing. ML: Methodology,
546 Funding acquisition, Project administration, Resources, Supervision, Writing—review
547 & editing.

548 **Funding**

549 This project received support from the CNRS, Toulouse University, and the European
550 Research Council (ERC Cog Bee-Move, grant number 101002644).

551 **Acknowledgments**

552 We thank all participants for their time and Renaud Bastien for early comments on
553 the manuscript.

554 **References**

- 555 1. C. H. Papadimitriou, The Euclidean travelling salesman problem is NP-
556 complete. *Theor Comput Sci* **4**, 237–244 (1977).
- 557 2. J. M. C. Hutchinson, G. Gigerenzer, Simple heuristics and rules of thumb:
558 Where psychologists and behavioural biologists might meet. *Behav Proc* **69**,
559 97–124 (2005).
- 560 3. J. N. Macgregor, T. Ormerod, Human performance on the traveling salesman
561 problem. *Percept Psychophys* **58**, 527–539 (1996).
- 562 4. B. M. Gibson, E. A. Wasserman, A. C. Kamil, Pigeons and people select
563 efficient routes when solving a one-way “traveling salesperson” task. *J Exp*
564 *Psychol Anim Behav Process* **33**, 244–261 (2007).
- 565 5. D. Vickers, P. Bovet, M. D. Lee, P. Hughes, The perception of minimal
566 structures: performance on open and closed versions of visually presented
567 Euclidean Travelling Salesperson Problems. *Perception* **32**, 871–886 (2003).
- 568 6. A. E. Cramer, C. R. Gallistel, Vervet monkeys as travelling salesmen. *Nature*
569 **387**, 464 (1997).
- 570 7. J. M. Wiener, N. N. Ehbauer, H. A. Mallot, Planning paths to multiple targets:
571 memory involvement and planning heuristics in spatial problem solving.
572 *Psychol Forsch* **73**, 644–658 (2009).

- 573 8. A. M. Reynolds, M. Lihoreau, L. Chittka, A simple iterative model accurately
574 captures complex trapline formation by bumblebees across spatial scales and
575 flower arrangements. *PLoS Comput Biol* **9**, 1–10 (2013).
- 576 9. J. Bureš, O. Burešová, L. Nerad, Can rats solve a simple version of the
577 traveling salesman problem? *Behav Brain Res* **52**, 133–142 (1992).
- 578 10. J. M. Wiener, A. Schnee, H. A. Mallot, Use and interaction of navigation
579 strategies in regionalized environments. *J Environ Psychol* **24**, 475–493 (2004).
- 580 11. J. M. Wiener, N. N. Ehbauer, H. A. Mallot, Path planning and optimization in the
581 traveling salesman problem: Nearest neighbor vs. region-based strategies. In
582 *Spatial Cognition: Specialization and Integration, Dagstuhl Seminar*
583 *Proceedings* **5491**, 1–21 (2007).
- 584 12. B. L. Golden, Empirical analysis of heuristics. *The traveling salesman problem*
585 218–222 (1985).
- 586 13. J. N. MacGregor, T. C. Ormerod, E. P. Chronicle, Spatial and contextual factors
587 in human performance on the Travelling Salesperson Problem. *Perception* **28**,
588 1417–1427 (1999).
- 589 14. C. Janson, “Spatial movement strategies: theory, evidence , and challenges”
590 in *On the Move: How and Why Animals Travel in Groups*, S. Boinski, P. A.
591 Garber, Eds. (University of Chicago Press., 2000), pp. 165–203.
- 592 15. J. A. Teichroeb, Vervet monkeys use paths consistent with context-specific
593 spatial movement heuristics. *Ecol Evol* **5**, 4706–4716 (2015).
- 594 16. C. Bellizzi, K. Goldsteinholm, R. E. Blaser, Some factors affecting performance
595 of rats in the traveling salesman problem. *Anim Cognit* **18**, 1207–1219 (2015).
- 596 17. M. Lihoreau, L. Chittka, S. C. Le Comber, N. E. Raine, Bees do not use
597 nearest-neighbour rules for optimization of multi-location routes. *Biol Lett* **8**,
598 13–16 (2012).
- 599 18. X. Kong, C. D. Schunn, Global vs. local information processing in visual/spatial
600 problem solving: The case of traveling salesman problem. *Cogn Syst Res* **8**,
601 192–207 (2007).
- 602 19. B. J. Best, “Modeling human performance on the traveling salesman problem:
603 empirical studies and computational simulations,” Carnegie Mellon Univ,
604 Pittsburgh, PA, USA. (2004).
- 605 20. S. M. Graham, A. Joshi, Z. Pizlo, The traveling salesman problem: A
606 hierarchical model. *Mem Cognit* **28**, 1191–1204 (2000).
- 607 21. R. Nori, M. M. Zucchelli, M. Palmiero, L. Piccardi, Environmental cognitive load
608 and spatial anxiety: What matters in navigation? *J Environ Psychol* **88**, 102032
609 (2023).

- 610 22. J. Wiener, T. Tenbrink, Traveling Salesman Problem: The Human Case. *KI* **22**,
611 18–22 (2008).
- 612 23. D. R. Montello, “Scale and multiple psychologies of space” in : Frank, A.U.,
613 Campari, I. (eds) *Spatial Information Theory A Theoretical Basis for GIS*.
614 COSIT 1993. Lecture Notes in Computer Science, vol 716. Springer, Berlin,
615 Heidelberg. https://doi.org/10.1007/3-540-57207-4_21 312–321 (1993).
- 616 24. R. E. Blaser, J. Wilber, A comparison of human performance in figural and
617 navigational versions of the traveling salesman problem. *Psychol Res* **77**, 761–
618 772 (2013).
- 619 25. A. Coutrot, *et al.*, Virtual navigation tested on a mobile app is predictive of real-
620 world wayfinding navigation performance. *PLoS One* **14**, e0213272 (2019).
- 621 26. J. Scherer, *et al.*, Not seeing the forest for the trees: combination of path
622 integration and landmark cues in human virtual navigation. *Front Behav*
623 *Neurosci* **18** (2024).
- 624 27. T. Wolbers, J. M. Wiener, Challenges for identifying the neural mechanisms
625 that support spatial navigation: the impact of spatial scale. *Front Hum Neurosci*
626 **8** (2014).
- 627 28. R. F. Wang, J. R. Brockmole, Human navigation in nested environments. *J Exp*
628 *Psychol Learn Mem Cognit* **29**, 398–404 (2003).
- 629 29. X. Han, S. Becker, One spatial map or many? Spatial coding of connected
630 environments. *J Exp Psychol Learn Mem Cognit* **40**, 511–531 (2014).
- 631 30. M.-L. Mittelstaedt, H. Mittelstaedt, Homing by path integration in a mammal.
632 *Naturwissenschaften* **67**, 566–567 (1980).
- 633 31. S. Heinze, A. Narendra, A. Cheung, Principles of insect path integration. *Curr*
634 *Biol* **28**, R1043–R1058 (2018).
- 635 32. T. D. Nguyen, *et al.*, Effects of scale change on distance perception in virtual
636 environments. *ACM Trans Appl Percept* **8**, 1–18 (2011).
- 637 33. T. Gärling, E. Gärling, Distance minimization in downtown pedestrian shopping.
638 *Env Plan A* **20**, 547–554 (1988).
- 639 34. C. F. Manski, Optimize, satisfice, or choose without deliberation? A simple
640 minimax-regret assessment. *Theory Decis* **83**, 155–173 (2017).
- 641 35. F. Lieder, T. L. Griffiths, Resource-rational analysis: Understanding human
642 cognition as the optimal use of limited computational resources. *Behav Brain*
643 *Sci* **43**, e1 (2020).
- 644 36. D. Kahneman, A. Tversky, Prospect theory: An analysis of decision under risk.
645 *Econometrica* **47**, 263 (1979).

- 646 37. Y. Xia, M. Manassi, K. Nakayama, K. Zipser, D. Whitney, Visual crowding in
647 driving. *J Vis* **20**, 1 (2020).
- 648 38. D. Whitney, D. M. Levi, Visual crowding: a fundamental limit on conscious
649 perception and object recognition. *Trends Cognit Sci* **15**, 160–168 (2011).
- 650 39. R. Misuraca, A. E. Nixon, S. Miceli, G. Di Stefano, C. Scaffidi Abbate, On the
651 advantages and disadvantages of choice: future research directions in choice
652 overload and its moderators. *Front Psychol* **15** (2024).
- 653 40. J. N. MacGregor, E. P. Chronicle, T. C. Ormerod, Convex hull or crossing
654 avoidance? Solution heuristics in the traveling salesperson problem. *Mem*
655 *Cognit* **32**, 260–270 (2004).
- 656 41. T. Tenbrink, J. Wiener, The verbalization of multiple strategies in a variant of the
657 traveling salesperson problem. *Cognit Proc* **10**, 143–161 (2009).
- 658 42. John. O’Keefe, Lynn. Nadel, *The hippocampus as a cognitive map* (Clarendon
659 Press □; Oxford University Press, 1978).
- 660 43. R. A. Epstein, E. Z. Patai, J. B. Julian, H. J. Spiers, The cognitive map in
661 humans: spatial navigation and beyond. *Nat Neurosci* **20**, 1504–1513 (2017).
- 662 44. S. L. Allison, A. M. Fagan, J. C. Morris, D. Head, Spatial Navigation in
663 Preclinical Alzheimer’s Disease. *J Alzheimer Dis* **52**, 77–90 (2016).
- 664 45. G. Coughlan, *et al.*, Test-retest reliability of spatial navigation in adults at-risk of
665 Alzheimer’s disease. *PLoS One* **15**, e0239077 (2020).
- 666 46. S. Tu, *et al.*, Lost in spatial translation – A novel tool to objectively assess
667 spatial disorientation in Alzheimer’s disease and frontotemporal dementia.
668 *Cortex* **67**, 83–94 (2015).
- 669 47. M. Peer, Y. Ron, R. Monsa, S. Arzy, Processing of different spatial scales in the
670 human brain. *Elife* **8**, e47492 (2019).
- 671 48. M. Lihoreau, L. Chittka, N. E. Raine, Trade-off between travel distance and
672 prioritization of high-reward sites in traplining bumblebees. *Funct Ecol* **25**,
673 1284–1292 (2011).
- 674 49. A. M. Reynolds, M. Lihoreau, L. Chittka, A simple iterative model accurately
675 captures complex trapline formation by bumblebees across spatial scales and
676 flower arrangements. *PLoS Comput Biol* **9**, e1002938- (2013).
- 677 50. E. Yavuz, *et al.*, Video gaming, but not reliance on GPS, is associated with
678 spatial navigation performance. *J Environ Psychol* **96**, 102296 (2024).
- 679 51. J. Brookes, M. Warburton, M. Alghadier, M. Mon-Williams, F. Mushtaq,
680 Studying human behavior with virtual reality: The Unity Experiment Framework.
681 *Behav Res Methods* **52**, 455–463 (2020).

- 682 52. M. M. Müller, *et al.*, The virtual navigation toolbox: Providing tools for virtual
683 navigation experiments. *PLoS One* **18**, e0293536 (2023).
- 684 53. S. Gillner, H. A. Mallot, Navigation and acquisition of spatial knowledge in a
685 virtual maze. *J Cogn Neurosci* **10**, 445–463 (1998).
- 686 54. E. A. Maguire, C. D. Frith, N. Burgess, J. G. Donnett, J. O’Keefe, Knowing
687 Where Things Are: Parahippocampal involvement in encoding object locations
688 in virtual large-scale space. *J Cognit Neurosci* **10**, 61–76 (1998).
- 689 55. J. Scherer, *et al.*, Not seeing the forest for the trees: combination of path
690 integration and landmark cues in human virtual navigation. *Front Behav*
691 *Neurosci* **18** (2024).
- 692 56. S. D. Moffat, S. M. Resnick, Effects of age on virtual environment place
693 navigation and allocentric cognitive mapping. *Behav Neurosci* **116**, 851–859
694 (2002).
- 695 57. R. E. Blaser, R. R. Ginchansky, Route selection by rats and humans in a
696 navigational traveling salesman problem. *Anim Cognit* **15**, 239–250 (2012).
- 697 58. M. Schrum, *et al.*, Concerning trends in Likert scale usage in human-robot
698 interaction: Towards improving best practices. *ACM Trans Hum Robot Interact*
699 **12**, 1–32 (2023).
- 700